Hail Impact Problem in Aeronautical Field.

Alessia Prato[1], Marco Anghileri[1], Luigi M.L. Castelletti[1]

[1] Politecnico di Milano, Dipartimento di Scienze e Tecnologie Aerospaziali, Milan, Italy

1 Introduction

Among soft body impacts, hail impact can be considered as one of the most dangerous, especially in aeronautical field. Even in the last month, some accidents occur because of hail impact. An example, in September 2014, an Airbus A330 from Madrid to Buenos Aires has been forced to land at the Ezeiza airport, near Buenos Aires, due to a hailstorm (Fig. 1).
The impact of hailstones against structures can have barely visible consequences, such as damage inside materials, especially in composite ones, or heavy consequences, from evident damage of the aircraft to fatal consequences for the passengers.

Fig.1: Hail impact: Airbus A330.

For all these reasons, a huge champagne of investigation on these phenomena has been done in the last years, especially from aircraft companies and research centers. Even if experimental tests are required to investigate the behavior of structural components subjected to hail impact, the use of numerical simulations becomes more and more important, especially for the predictive possibility of investigation of complex impact scenario.
Explicit finite element codes allow modeling the hailstone using different approach. The historically most used is the Lagrangian (LAG) approach but the high distortion of elements caused numerical instabilities till the bad termination of the analysis. The Smoothed Particle Hydrodynamics (SPH) technique is also used but it presents some limits. To overcome these problems, some explicit codes have recently implemented a new technique that allow to switch from LAG to SPH approach as the distortion of the lagrangian elements increase or as a failure criteria is imposed to the finite elements (FE).
Few research works have been performed using this method and applied it to the study of different material such as aluminum (Plassard et al. in [1]) or soil behavior (Kulak and Bojanowski in [2]). Some numerical models have been performed not only using LS-DYNA (Beal et al. in [3]) but also using other explicit finite element codes, like ABAQUS/Explicit (Zahedi et al. [4])
In this paper, an investigation of the hail impact phenomena under a numerical point of view is presented. After a short description of different hail models, a comparison among them has been done. Two different case studies are also proposed: an investigation of the effect of different target materials and a single/multiple hail impact against a complex structure. As a result of this investigation, some general considerations on the argument are here presented.

2 Hail numerical models

Hail impact has been investigated from rather long time. Many research centers presented numerical studies on this argument. Kim at al. analyzed the impact of hail against target structures of different materials and numerical model results have been validated throughout experimental tests [5, 6]. Sanchez et al. in [7] and Anghileri et al. in [8] proposed different hail discretizations: from LAG to EFG and SPH.

In this paper a simple spherical hail stone impacting on an aluminum plate, 2mm thick, is considered. An initial impact velocity of about 60.6 m/s has been used. The material adopted for the hail model is the one proposed by Kim, see Tab. 1.

Property	Value
Mass density - kg/m^3	846
Shear modulus – Mpa	3460
Yield stress – Mpa	10.3
Plastic Hardening Modulus - MPa	6890
Bulk modulus – MPa	8990
Plastic failure strain- %	0.35
Ultimate Tensile Stress - MPa	-4

Table 1: Ice material property

2.1 Lagrangian approach

The LAG approach has been historically the first used to investigate components. It is useful to study nonlinear problems but as the deformation of the elements increases, inaccuracy problems can occur, as the related computational costs. This approach has been used for the study of the mesh dependency of a hailstone. Even if the nominal dimension of the elements is the same (2 mm), the internal geometry of the hail has been modeled in different ways. Both Hexa and Tria elements have been considered (Fig. 1)

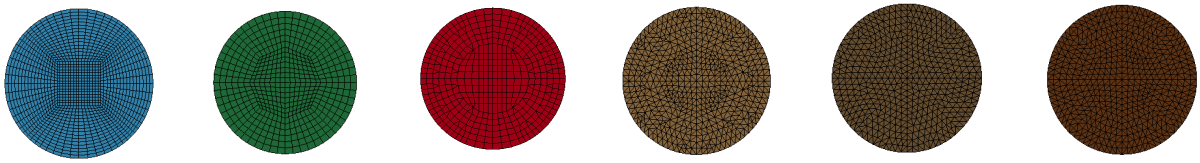

Fig. 2: Lagrangian model: Mesh1 (blue), Mesh2 (green), Mesh3 (red); Tria1 (beige), Tria2 (light brown), Tria3 (brown).

From a qualitative point of view, the behavior of the hail against the plate for the hexa elements is in accordance with the hydrodynamic theory, considering instead of a cylindrical geometry a spherical one. The pressure distribution is almost the same for all mesh models (Fig.3).

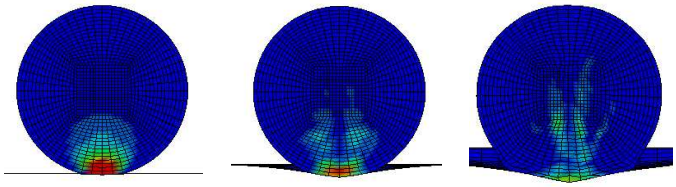

Fig. 3: Lagrangian model: pressure distribution of the hail model (Mesh1) for different instants of time.

A comparison of the contact forces of the three Hexa models demonstrates a good correspondence in the model results, even if small differences occurs (Fig. 4).

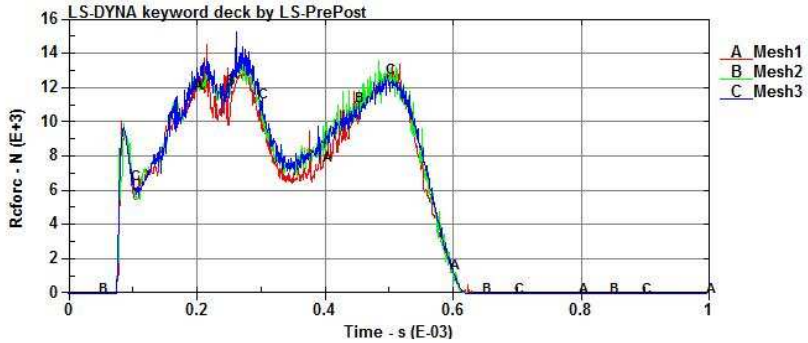

Fig. 3: Lagrangian model: contact force in the Hexa models.

The differences in results mainly depend on the fact that Mesh1 is less homogeneous then the others and, in the central part of the hail, the dimension of some elements is equal to half the nominal one.
Referring to the Tria meshes, due to the element geometry, a high element distortion during the final instant of impact is shown (Fig.4).

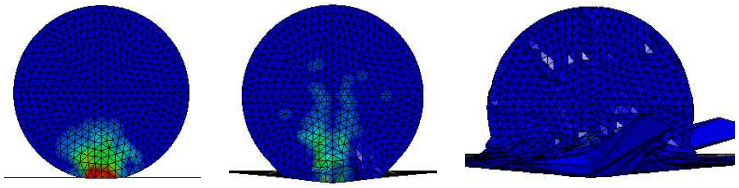

Fig. 4: Lagrangian model: pressure distribution of the hail model (Tria2) for different instants of time.

From a comparison of the contact forces in the Tria models, the inaccuracy caused the non stable trend of the curves in the final instants of the simulations, till the “error termination” of the models (Fig.5).

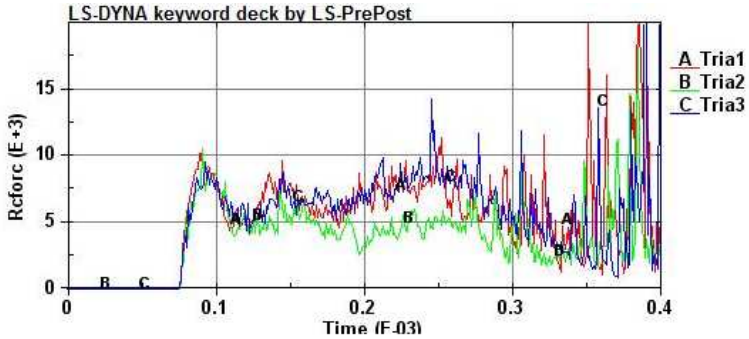

Fig. 5: Lagrangian model: contact force in the Tria models.

2.2 SPH approach

The Smoothed Particle Hydrodynamics approach (SPH) was also adopted to discretise the hail model. The main advantages is the use of particles, instead a grid, as a computational framework on which the problem is solved. This approximation allows obtaining higher distortion in the hail model during the impact against a target structure. The target structure, the initial and boundary conditions adopted for the simulations are the same presented for the LAG model.
The spatial distribution of the particles (Fig.6) inside the hail geometry varies from one point for each finite element (Sph1, Sph2, SPh3) to an uniform distribution of the particles inside the volume (Sph4 and Sph5). The first three distributions are obtained starting from the corresponding lagrangian descriptions (from Mesh1 to Mesh3).

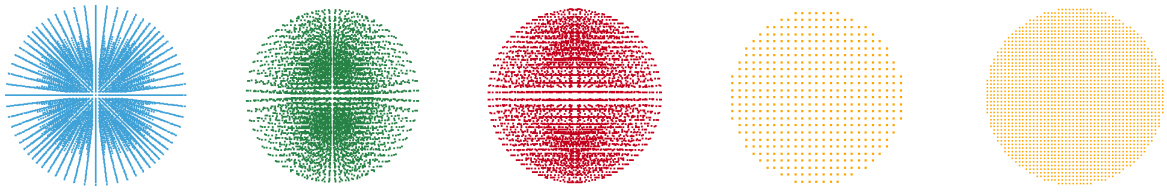

Fig. 6: SPH model: particles distribution Sph1 (blue), Sph2 (green), Sph3 (red), Sph4 (yellow), Sph5 (yellow).

The pressure distribution inside the hail can be easily compared to the one presented for the Mesh1 solution (Fig. 7).

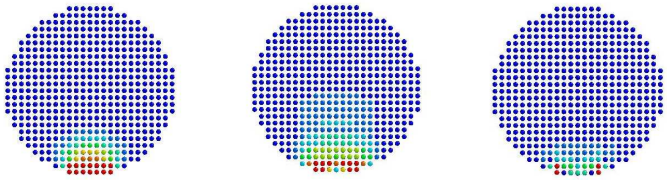

Fig. 7: SPH model: pressure distribution of the hail model (Sph5) for different instants of time.

A comparison between the different SPH models has been performed in term of contact forces (Fig. 8). A good agreement in the trend of the curves is demonstrated even if some differences can be shown. They are related to the particle distribution. The presence of delayed first peak of forces is due to a non homogeneous distribution of particles. This is more evident for Sph1 in which there is a concentration of particles at the centre of the hail.

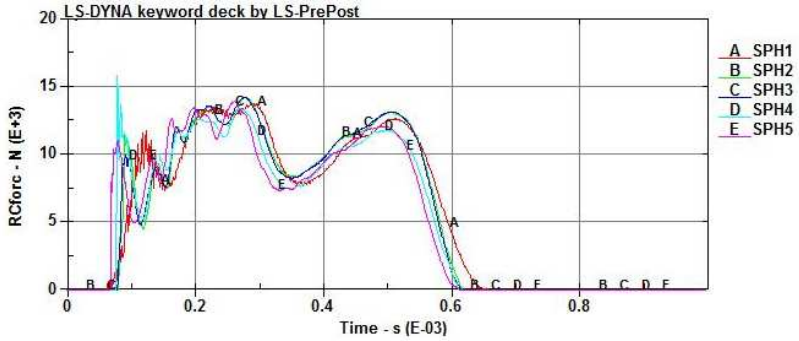

Fig. 8: SPH model: contact force.

2.3 FE-to-SPH approach

The third approach here proposed is the FE-to-SPH one. Starting from a LAG model, as solid elements failed, they are transformed into SPH particles, avoiding in this way the high distortion of the grid during the impact. The number of the particles for each lagrangian element is a used defined parameters. Properties, materials and contacts can be defined both for solid elements and SPH particles.
To switch from LAG to SPH, a control card ***ADAPTIVE_SOLID_TO_SPH** has been used [9, 10, 11]. Because of a more homogeneous distribution of elements, the Mesh2 and Mesh3 model have been adopted (Fig. 9).

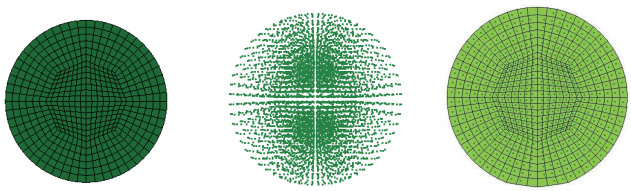

Fig. 9: FE-to-SPH model: FEtoSPH2 (green) and FEtoSPH3 (red) compared with the corresponding LAG and SPH discretizations.

The analysis of the pressure distribution inside the hail demonstrates that the behavior is mainly governed by the LAG model (Fig.10).

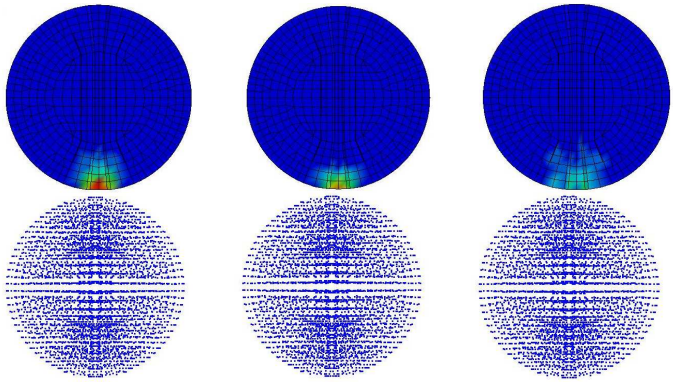

Fig. 10: FE-to-SPH model: pressure distribution of the lagrangian part and the SPH one of the model (FEtoSPH2) for different instants of time.

This behavior is more evident comparing, for FEtoSPH3, the contact force of the lagrangian part and of the SPH one with the total contact force (Fig. 11). A similar consideration can be done also plotting together the contact force of the pure lagrangian (Mesh3) and pure SPH (Sph3) models with this new approach, for which the general trend of the curve is almost the same of the lagrangian one (Fig.12).

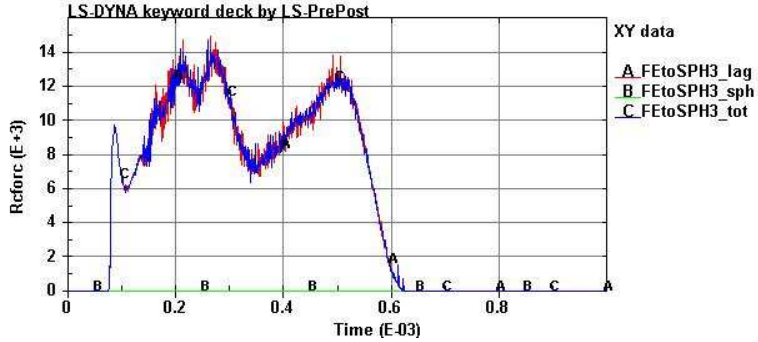

Fig. 11: FE-to-SPH model: contact force (FEtoSPH3).

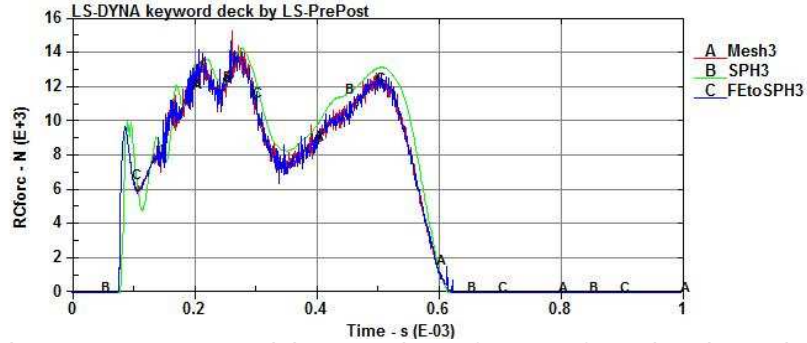

Fig. 12: FE-to-SPH model: comparison of contact force (Mesh3, Sph3, FEtoSPH3).

If a failure criteria is activated, the erase of the lagrangian element allow increasing the contribution of the SPH component. This fact can be shown considering both the distribution of the pressure inside the hail, for the lagrangian and SPH part (Fig.13), and from the comparison of the contact force contributions (Fig. 14 and Fig.15).

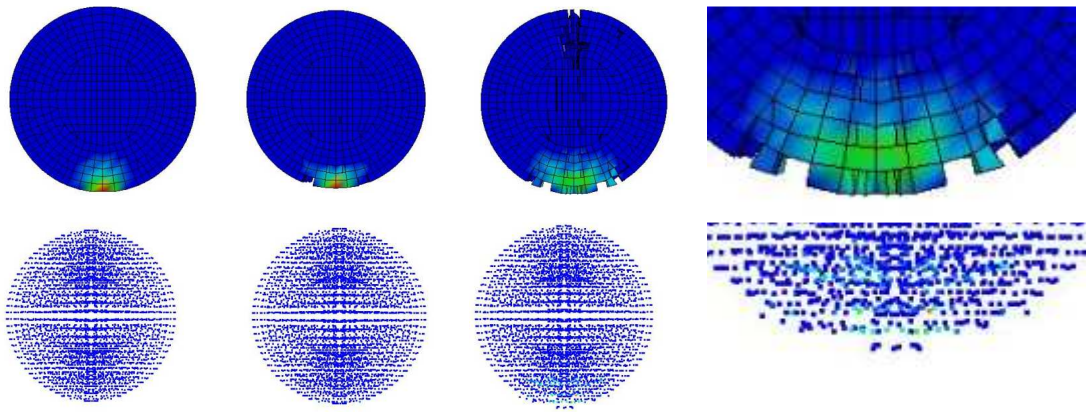

Fig. 13: FE-to-SPH model: comparison of pressure distribution of the LAG part and the SPH one for different instants of time with a detail of the contact region.

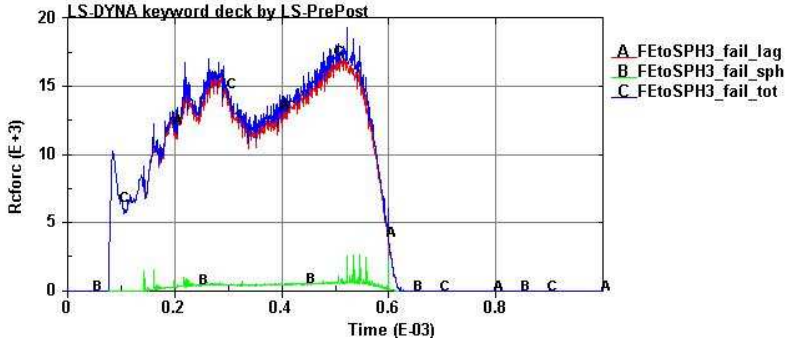

Fig. 14: FE-to-SPH model: contact force (FEtoSPH3_fail).

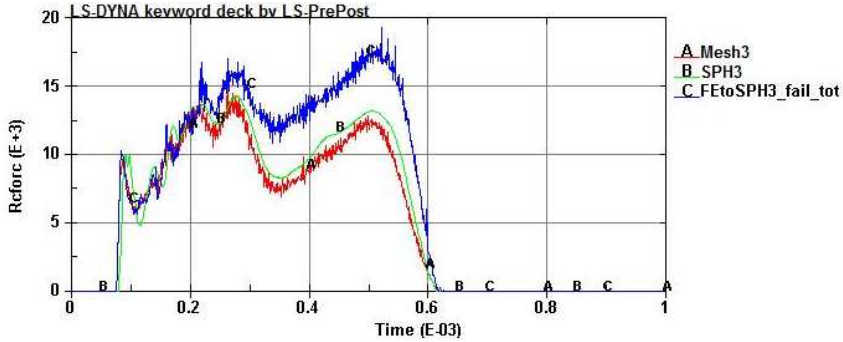

Fig. 15: FE-to-SPH model: comparison of contact force (Mesh3, Sph3, FEtoSPH3_fail).

2.4 Conclusions

This investigation on the effect of the use of different approach to model the hailstons has a relevant rule in the study of the optimal method to be used to reproduce real impact event.
The use of an opportune and sufficiently homogeneous discretization of the mesh, or distribution of the SPH particles, allow to reduce instability problems. The high deformation of the elements causes a wrong behavior of the model, respect to the Hexa ones, and a high computational cost till the “error termination” problems for Tria mesh.
From the comparison of a FE-to-SPH model with and without the activation of the failure of lagrangian elements, if a failure criterion is not used, the behavior of the new approach is almost the same of the lagrangian one. If a failure criteria is instead applied, the behavior of the new model in terms of contact force differ from the lagrangian due to the SPH contribution and to the formulation itself (Fig. 14 and

15). A proper calibration of the hail definition, especially hail material model, for the FE-to SPH model can be required for a correct correlation of the events.

3 Case study 1: effect of the target material

After the discussion on possible discretization of the hail, a study on different materials used for the target structures is here presented. From the comparison of LAG, SPH and FE-to-SPH approaches, the hail model used for this case study has been the SPH2 one because of a not so high computational cost and a good agreement with Lagrangian results, respect to the FE-to-SPH one. The hail geometry and material model and the boundary conditions are the same previously presented. Also the geometry of the target structure is the same. The plate has been made using four different materials: aluminum, carbon fibers composite, a kevlar fibers composite and a glass fibers one. The mechanical properties of the material adopted in this study have been investigated in previously research works and the numerical material models have been assessed throughout experimental tests. Six impact velocities have been used in order to evaluate the change in target displacement and contact force as the velocity increase. After an introduction on material models applied, the effect of the velocity for each material is presented. As a conclusion, some regression curves are here shown to generalize the material effect as the velocity changes.

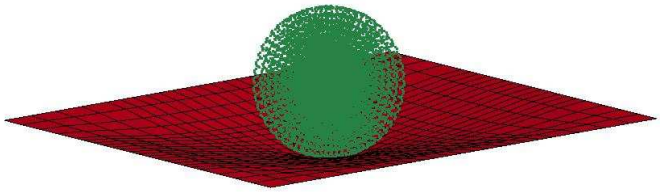

Fig. 16: Effect of target material: Sph2 hail model impacting an aluminum plate.

3.1 Aluminum material models

The target plate has been made in Al2014 aluminum alloy. The material model used for the finite element analysis has been the ***MAT_PIECEWISE_LINEAR_PLASTICITY** one. This is an elasto-plastic one with a used defined stress-strain curve and for which a strain-rate dependency can be applied.
As previously said, a Sph2 hail model impacted the aluminum plate with six different initial velocities: 25 m/s, 50 m/s, 75 m/s, 100 m/s, 150 m/s and 200 m/s. Results in terms of contact forces and displacement, as function of time, are shown in Fig. 17 and Fig. 18.

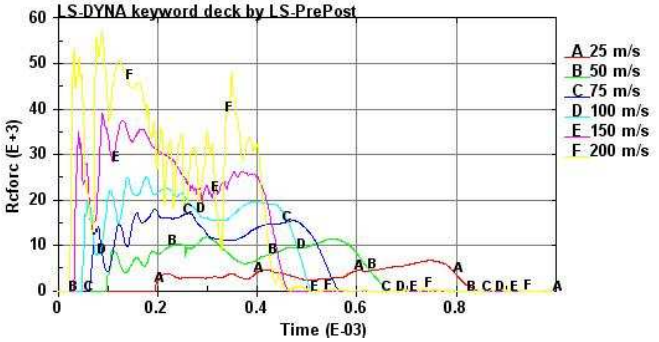

Fig. 17: Effect of target material: aluminum plate (contact force).

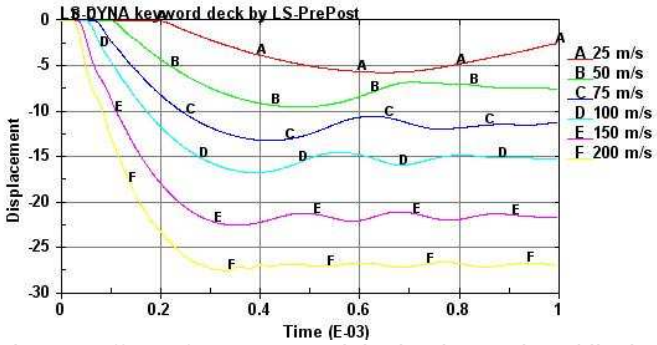

Fig. 18: Effect of target material: aluminum plate (displacement).

From results, an increase in the peak of force and in displacement, as the velocity increase, is shown. A delay in the dynamic of the event is also shown due to the decrease of the initial velocity. This effect is more evident in Fig. 17.

3.2 Carbon fibers composite material models

An eight layers composite panel has been also considered. The stack sequence applied for all the composite target structures here presented is a $[0,+45,90,-45]_{sym}$. To model the composite in LS-DYNA, the ***PART_COMPOSITE** and ***MAT_LAMINATED_COMPOSITE_FABRIC** has been used. This material is described in detail in [12]. It allows modeling both unidirectional, woven fabric and complete laminate. Failure modes of the composite are considered.
Referring to the carbon composite one, each lamina presents a tissue structure made with high performances/intermediate modulus carbon fibers and an epoxy matrix.
As previously said, six impact velocity has been considered. Results referring to the contact forces (Fig. 19) and displacements (Fig.20) are here shown.

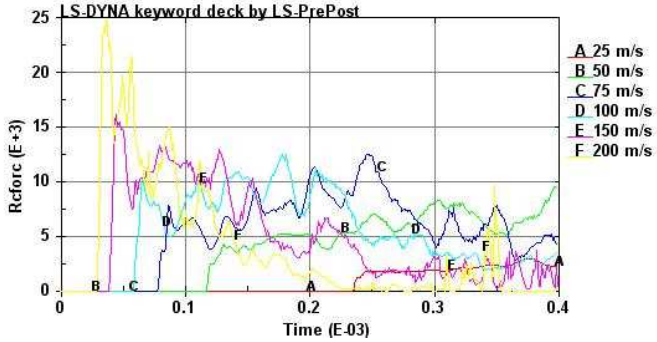

Fig. 19: Effect of target material: carbon fibers composite plate (contact force).

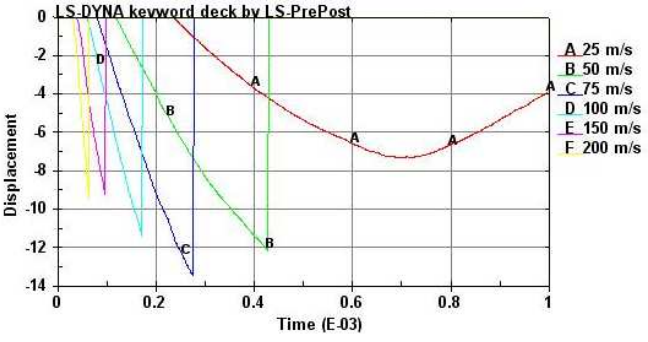

Fig. 20: Effect of target material: carbon fibers composite plate (displacement).

The increase of the peak of force as the velocity increase was shown. Differences respect to the aluminum case are presented in Fig. 20. For an initial velocity of 25 m/s, the thin composite plate does not break, instead for increasing velocity, the displacement of the central node of the plate reaches a maximum value around 10 mm before the elements at the center of the target break. The earlier break of the plate is relate to the highest impact velocity, as expected (Fig. 20).

3.3 Kevlar fibers composite material models

A composite material made with kevlar intermediate modulus fibers was also considered. The ***PART_COMPOSITE** and ***MAT_LAMINATED_COMPOSITE_FABRIC** has been used also in this case to model the material in LS-DYNA. The lamination sequence is the same presented for the carbon fibers composites. All the informations previously presented for the hail model, for the boundary conditions and for the impact velocities have been used also in this case.
As shown in Fig. 21, the contact force curves present a similar trend referring to what shown for the composite case.

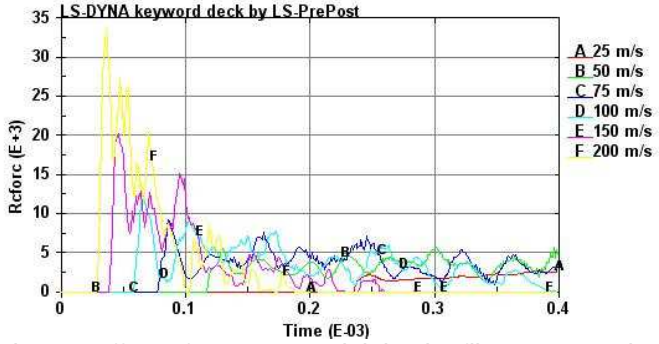

Fig. 21: Effect of target material: kevlar fibers composite plate (contact force).

The maximum displacement of the central node of the plate decreases as the impact velocity increases due to the plate damage. From a comparison of the 25 m/s curve for carbon fibers and kevlar, a rupture of the kevlar target is shown even if the maximum displacement values are not so different.

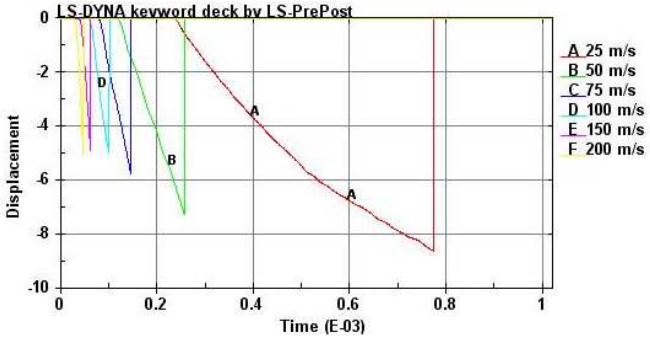

Fig. 22: Effect of target material: kevlar fibers composite plate (displacement).

3.4 Glass fibers composite material models

The last material considered in this case study is a glass fibers fabric prepreg composite one. As previously done, ***PART_COMPOSITE** and ***MAT_LAMINATED_COMPOSITE_FABRIC** has been used to model the 8 layers symmetrical composite structure. Results of the contact forces and displacements as functions of time and velocity are here presented.

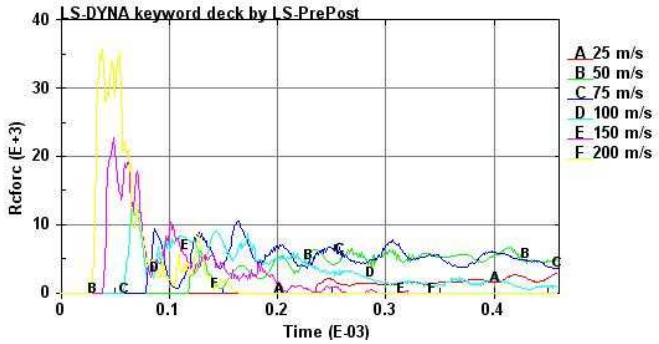

Fig. 23: Effect of target material: glass fibers composite plate (contact force).

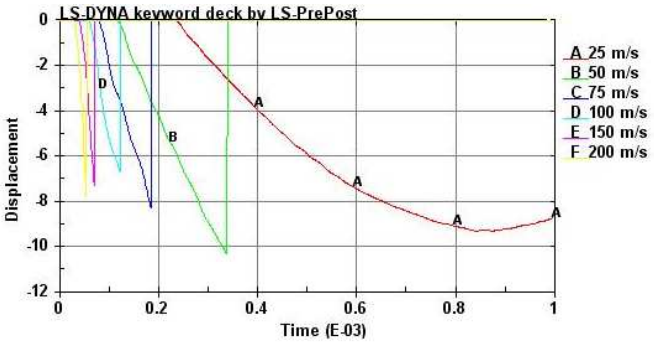

Fig. 24: Effect of target material: glass fibers composite plate (displacement).

Results presented in Fig. 23 and Fig. 24 allow considerations similar to what presented for the carbon composite material target plate. Differences in peak force and displacement values are related to the material models.

3.5 Conclusions

To have a more general perspective on the behavior of the target structure materials as the initial impact velocity change, a final comparison is here presented. In Fig 24 the maximum value of the contact forces obtained for each material is shown. This values seem to be higher for the aluminum plate respect to the composite one probably because of the failure of the composite target structure as the hail impacted it. No great differences seem to be among the composite materials in the trend of the curve.

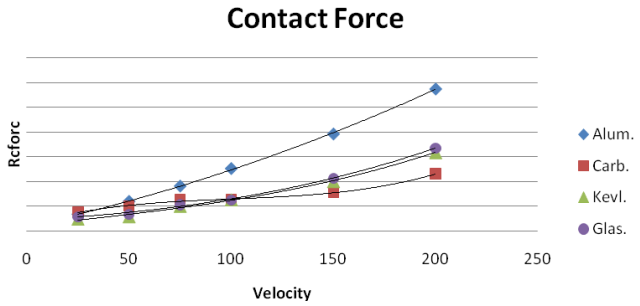

Fig. 25: Effect of target material: comparison of contact forces.

Similar considerations can be done from the comparison of the displacement of the central point of the plate. As shown before, the presence of a higher displacement in the aluminum plate is strictly related to the plastic deformation of the target. The increase of the displacement can be described using a power law function. Instead, referring to the composite ones, if a small increase of displacement can be shown for low velocity impact, as the velocity increase, the earlier damage of the plate caused a small deformation of the structure before the failure till the reach of an almost stable value of displacement (Fig. 26). For composite materials, a polynomial function seems to better describe the trends of the displacements.

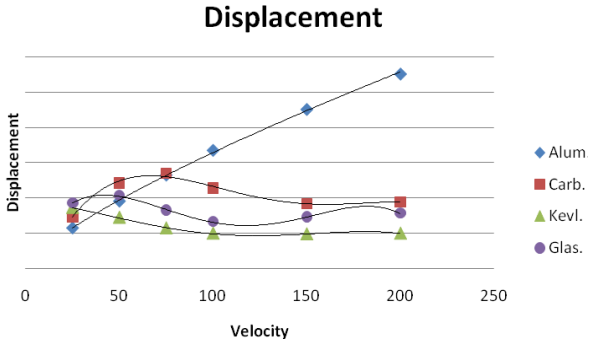

Fig. 26: Effect of target material: comparison of displacements.

A better investigation on this argument must be considered. Experimental tests, with constant hail geometry, target thickness and boundary conditions, are required to evaluate and understand the effect of the material.

4 Case study 2: Single and multiple hail impact against a complex target structure

In this second case study, a single and multiple hail impact against a complex target structure are proposed. From what previously said, the hail has been modeled using Sph3 ones. The target is made in aluminum alloy. A comparison in terms of hail and structure deformation and contact force is here presented.

4.1 Single hail impact

The hail material is the one presented in Table 1 (***MAT_ELASTIC_PLASTIC_HYDRO_SPALL).** The target structure is the frontal part of an engine and has been modelled using the ***MAT_PIECEWISE_LINEAR_PLASTICITY** card. The initial impact velocity of the hail has been of 180 m/s. A contact has been defined between the hail and the engine. Boundary conditions have been imposed in the back part of the target.

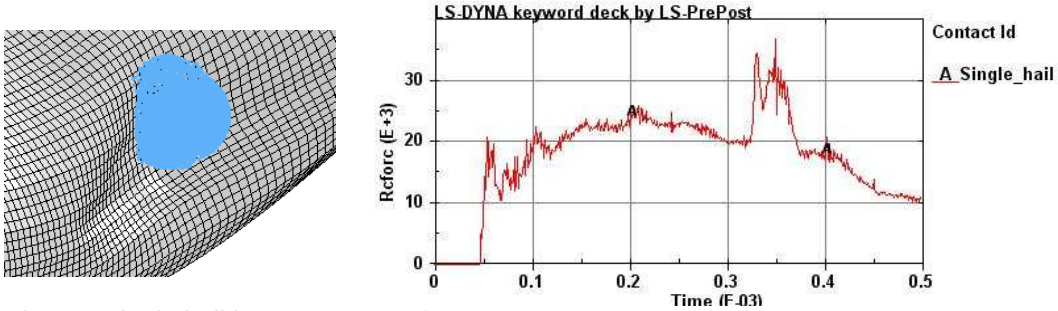

Fig. 27: Single hail impact: contact force.

From results it's possible to see that the contact force curve presents two peaks of forces, the second is related to the deformation of the target structure.

4.2 Multiple hail impact

A multiple hail impact has been also considered. Three hails impacted at 180 m/s a small portion of the engine. The deformation of the structure and the contact force due to the impact is presented in Fig. 28.

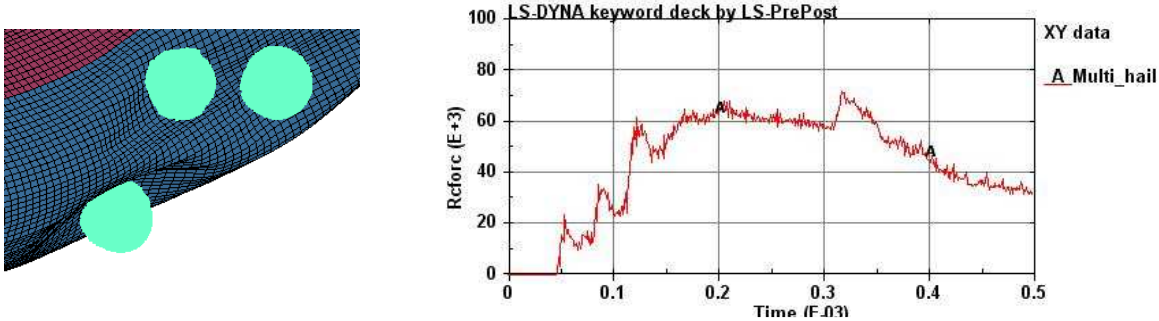

Fig. 28: Multiple hail impact: contact force.

4.3 Conclusions

From a comparison of the contact curve results, it can be shown that the value of the force is almost linearly dependent to the number of the impacting structures but some differences are due to the deformation of the target structure and of the impacting objects (Fig. 29). The global trend is almost the same but in the multi hail curve, the first three peaks of force are related to the impact of each hailstones.

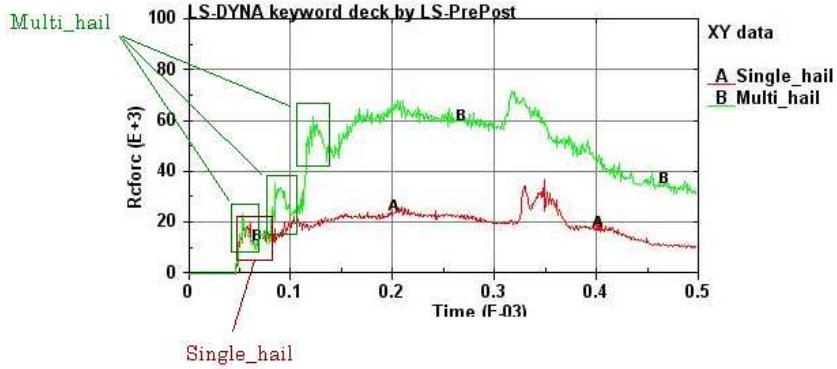

Fig. 29: Comparison of contact force: single and multiple hail impact.

For completeness, the correspondent multiple hail impact lagrangian model has also been done in order to verify the good correlation between the two approaches used to model the hail if applied to a complex problem. As presented in Fig. 30, only small differences are shown, as previously observed in Fig. 13.

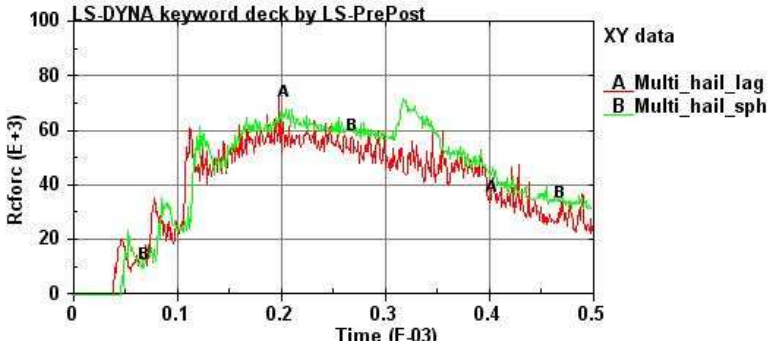

Fig. 30: Comparison of contact force: SPH and LAG model.

5 Conlusions and future works

In crashworthiness, soft body impact has a central rule especially in aeronautical field. Studies on hailstones have been performed both experimentally and numerically, using explicit finite element codes. In this research work, benefit and drawback of different approaches have been presented.
To evaluate the better solution to model hailstones, the use of SPH particles has been compared to Lagrangian model and the new FE-to-SPH one. Few differences have been shown from LAG and SPH in terms of contact forces and internal pressure of the hail. Some differences have been instead demonstrated referring to the FE-to-SPH model due to the failure activation option.
Using the SPH hail definition, a comparison on the impact against plates made in different material have been presented in Case Study 1. From results the maximum contact force and displacement have been plotted for each material as a function of the velocity and regression curves have been shown.
In Case Study 2, a single and multiple hail impact against an aeronautical engine is presented. Contact forces and structure deformation have been compared and the agreement in results between lagrangian and SPH case has been demonstrated also in a more complex case.
A further investigation on this phenomenon is required, especially the use of experimental tests for the validation of numerical models of hail (see FE-to-SPH one) and of target structure.

6 Literature

[1] Plassard F., Mespoulet J., Hereil P., “Hypervelocity impact of aluminium sphere against aluminium plate: experiment and LS-DYNA correlation”, 8th European LS-DYNA conference, Strasbourg, 2011

[2] Kulak R. F., Bojanowski C., “Modeling of Cone Penetration Test Using SPH and MM-ALE Approach”, 8th European LS-DYNA conference, Strasbourg, 2011

[3] Beal T., Van Dorsselaer N., Lapoujade V., “A contribution to validation of SPH new features”, 9th European LS-DYNA conference, Manchester, 2013

[4] Zahedi S.A., Demiral M., Roy A., Silberschmidt V. V., “FE/SPH modelling of orthogonal micro-machining of f.c.c. single crystal”, Computational Materials Science, Vol 78, 2013, p. 104-109

[5] Kim H., Kedward K.T., “Modeling hail ice impacts and predicting impact damage initiation in composite structures”, AIAA Journal, Vol. 38, 2000

[6] Tippmann J. D., Kim H., Rhymer J. D., “Experimentally Validated Strain Rate Dependent Material Model for Spherical Ice Impact Simulation”, International Journal of Impact Engineering, Vol. 57, 2013, p. 43-54

[7] Sànchez, J.P., Pedroche D. A., Varas D., Lòpez-Puente J., Zaera R., “Numerical modeling of ice behavior under high velocity impacts”, International Journal of Solids and Structures, Vol. 49, 2012, p. 1919-1927

[8] Anghileri M., Castelletti L. M. L., Milanese A., Semboloni A., “Modeling Hailstone Impact onto Composite Material Panel Under a Multi-axial State of Stress”, 6th European LS-DYNA User’s Conference, Gothenburg, 2007

[9] Livermore Software Technology Corporation, LS-DYNA Keyword User's Manual Vol 1, Version 971 R6.1.0, August 2012

[10] Livermore Software Technology Corporation, LS-DYNA Keyword User's Manual Vol 2, Version 971 R6.1.0, August 2012

[11] Livermore Software Technology Corporation, LS-DYNA Theory Manual, March 2006

[12] Matzenmiller A., Lubliner J., Taylor R.L.: “A constitutive model for anisotropic damage in fiber-composites”, Mehanics of Material, Vol. 20, 1995, p. 125-152